SAND2009-3287P

Alpha79i Neutron Cross-Section Library Performance Testing

John Mattingly, Sandia National Laboratories

Glenn Sjoden and Ce Yi, University of Florida

11 May 2009

Introduction

The University of Florida Department of Nuclear and Radiological Engineering (UF) is conducting a joint study with Sandia National Laboratories to identify deterministic neutron transport techniques that optimally balance computational speed with accuracy for the purposes of computing neutron multiplicity metrics. A key element in this study is identifying cross-section library generation techniques that minimize computational time. Factors affecting computational time include:

- The number of energy groups
- The order of the scatter matrix Legendre polynomial expansion
- The number of upscatter groups in the scatter matrix

Generally, coarser energy group structures, lower-order scatter matrix Legendre expansions, and fewer upscatter groups result in shorter computational times. However, performance enhancements gained by minimizing these parameters can negatively impact computational accuracy.

As a first step toward developing a cross-section library that optimally balances computational speed and accuracy, UF is working to develop a library that will serve as a baseline for subsequent evaluations of alternative libraries. The principal criterion for choosing a "baseline" library is that it matches or exceeds the computational speed and accuracy of the Kynea3 library developed by Sandia (Varley and Mattingly 2008).

UF has been experimenting with a series of cross-section libraries named "Alpha79." This report summarizes tests conducted on the ninth revision of that library, Alpha79i.

Alpha79i, like all the Alpha79-series libraries, was collapsed from the SCALE 238-group library (Bowman et al., 2006). The weighting function used to collapse the SCALE 238-group library onto the Alpha79 group structure is shown in Figure 1. In the figure, the Alpha79i weighting function is compared to the weighting function that was used to collapse the VITAMIN-B6 199-group library (White et al., 1994) onto the Kynea3 group structure. Both weighting functions exhibit the Maxwellian distribution at low energy, with a "$1/E$" continuous slowing down spectrum at intermediate energies, followed by a Watt fission spectrum at high energy. This composite spectrum is typically observed in moderated fissile metals.

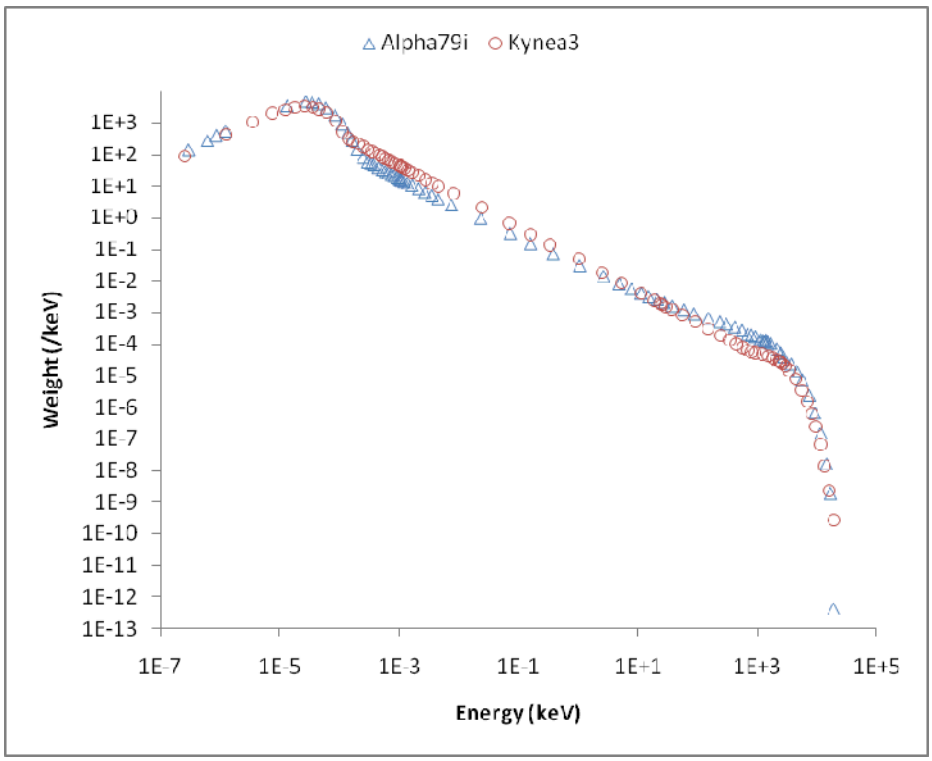

Figure 1: Alpha79i and Kynea3 spectral weighting functions

Both the Kynea3 and Alpha79-series libraries contain similar numbers of upscatter groups in their respective scatter matrices. The SCALE 238-group library provides fifth-order Legendre polynomial (i.e., P5) expansions of the scatter matrix, while the VITAMIN-B6 library provides seventh-order (P7) expansions. Consequently, the Kynea3 library has the potential to more accurately solve problems characterized by scattering that is highly peaked in the forward direction (as is exhibited by some deep penetration problems.) However, tests conducted on an earlier Alpha79 revision, Alpha79g, showed that for the class of problems being studied, namely fissile metals moderated by hydrogenous reflectors, P5 is sufficient. This was established by comparing Feynman-Y estimates obtained using the Alph79g library, the standard P7 version of the Kynea3 library, and a P5 version of the Kynea3 library. One such comparison is shown in Figure 2. The source for the case shown ("berp4") was the BeRP ball reflected by 7.6 cm of polyethylene (Valentine 2008). The result shown in the figure is typical – the difference between P5 and P7 is slight. In some cases, the difference is insubstantial.

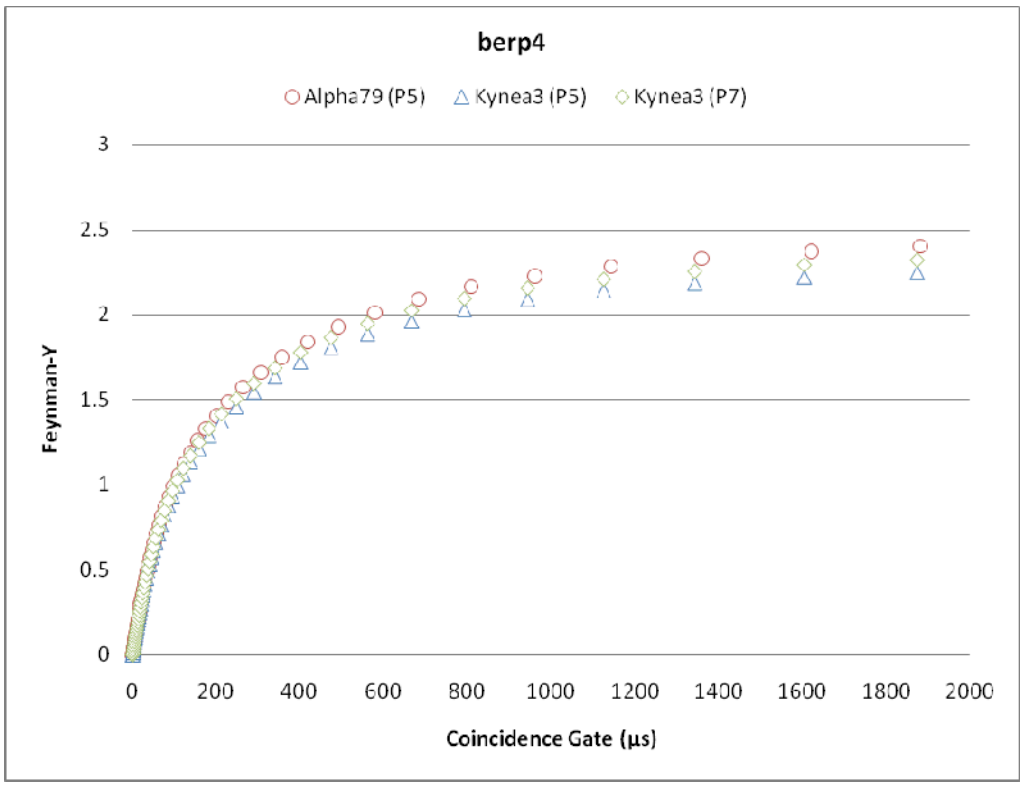

Figure 2: Feynman-Y estimates obtained using the Alpha79g library, a P5 version of the Kynea3 library, and the standard P7 version of the Kynea3 library

The Alpha79i library was subjected to several tests to compare it to the current Kynea3 library. If calculations performed using the Alpha79i library exhibit accuracy and speed similar to calculations using the Kynea3 library, then Alpha79i can be used as a baseline for evaluating subsequent libraries for relative improvements in computational performance.

Tests Conducted

One-dimensional transport models of the BeRP ball reflected by spherical shells of polyethylene were run using the Kynea3 and Alpha79i libraries. The radial thickness of the polyethylene spherical shells varied from 0 (i.e., no reflector) to 152.4 mm. The calculations included forward and adjoint time-independent transport and forward time-dependent transport, which are all used to compute the Feynman-Y versus coincidence gate width for a neutron multiplicity counter. Coupled neutron-gamma calculations were also performed to compute the contribution of (n, γ) and (n, n') reactions to the gamma spectrum. The Los Alamos code PARTISN was used to solve the neutron transport equation. The Sandia code ONELD was used to solve the photon transport equation.

Test Results

Several metrics were used to compare the solution obtained using each library. These metrics included:

- The effective neutron multiplication factor k (k-effective), and the neutron multiplication $M = 1/(1-k)$.
- The neutron count rate computed for a portable multiplicity counter, the NPOD developed at Los Alamos National Laboratory. The count rate R was computed by folding the neutron leakage current J with a model for the NPOD's detection efficiency $\dot{o}$ versus energy E, i.e., $R = \int dE\, \dot{o}(E)\, J(E)$. Note that this is actually an inner product between the neutron flux φ and the detector cross section Σ_d, i.e., $R = \int dr \int dE \int d\Omega\, \Sigma_d(r,E,\hat{\Omega})\, \varphi(r,E,\hat{\Omega})$, where the detector cross section has been represented as an efficiency for neutrons escaping the outer surface of the transport medium, i.e., where $\Sigma_d(r,E,\hat{\Omega}) = \hat{n}\cdot\hat{\Omega}\, \delta(r \in \mathrm{S})\, \dot{o}(E)|_{\hat{n}\cdot\hat{\Omega}>0}$ for where $\hat{n}$ is the normal to the problem outer boundary S and $\hat{\Omega}$ denotes direction.
- The ratio of the count rate computed using the leakage current J and detector efficiency $\dot{o}$ to the count rate computed using the adjoint flux $\varphi^{\dagger}$ and the forward source term Q, i.e., the ratio $\int dE\, \dot{o}(E)\, J(E) \Big/ \int dr \int dE\, \varphi^{\dagger}(r,E)\, Q(r,E)$. Nominally, this ratio should be unity as dictated by the commutation relation between the forward and adjoint solutions.
- The asymptotic value of the Feynman-Y. The formula for the Feynman-Y asymptote is documented in (Mattingly and Varley 2008).

These metrics are summarized in Table 1. The k-effective (and multiplication) computed for each case is compared to estimates reported in Valentine's subcritical benchmark (Valentine 2008).[1] These comparisons are also shown in Figure 4 through Figure 7. The apparent under-prediction of k-effective for the lightly reflected cases may be due to the experimental setup Valentine used. It employed two large blocks of polyethylene as detector moderators, and these may have increased the k-effective of the BeRP ball via neutron feedback. Alternatively, both the Kynea3 and Alpha79h cross-section libraries may actually under-predict k-effective for lightly moderated sources due to their weighting functions. These observations are discussed later in this section.

In previous tests of the Alpha79 library, an empirical model of neutron detection efficiency model was used. That model was obtained via a procedure that unfolds detection efficiency versus energy from a handful of neutron count rate measurements. (Harding, Mattingly and Mitchell 2008) However, it was speculated that the empirical model of detection efficiency introduced error into the calculations of the neutron count rate and of the Feynman-Y. To confirm that theory, the empirical model of detection efficiency was replaced by one computed using MCNP. (Mattingly 2009)

The detection efficiency calculated by MCNP differs substantially from the empirical model as Figure 3 illustrates. In particular, the MCNP calculation shows that the cadmium cutoff is much sharper than estimated by the empirical model. Also, the MCNP calculation is less flat between the lower and upper

[1] Note that Valentine's benchmark did not estimate k-effective for the case where the reflector thickness was 152.4 cm.

thresholds than predicted by the empirical model. The "wiggles" evident in the MCNP calculation result from resonances in the cadmium absorption cross section.

In general, using the detection efficiency calculated by MCNP in place of the empirical model substantially improved the accuracy of nearly every calculation.

The computed neutron count rate is compared to measurements conducted in January 2009 (Mattingly 2009) in Table 1 and in Figure 8 and Figure 9. Overall, calculations using either the Kynea3 or the Alpha79i library tend to correctly predict the measured count rate. The Alpha79i library tends to over-predict the measured count rate very slightly for the most heavily moderated cases, berp4 and berp5.

As shown in Figure 10 and Figure 11, the Alpha79i library tends to over-predict the Feynman-Y asymptote relative to the Kynea3 library. This is also evident in Figure 12 through Figure 17.

With the introduction of the MCNP-calculated detection efficiency model, the Kynea3 Feynman-Y calculations now tend to match the measurements with nearly acceptable accuracy. The remaining discrepancies in the Kynea3 calculations are probably still due to the detection efficiency model: the MCNP calculation did not include the floor, which will impact the detection efficiency, particularly for the bare BeRP ball.

The discrepancies evident in the Alpha79 calculations are most probably due to the way in which the plutonium cross sections were collapsed from the SCALE 238-group library. The effect is evident in Figure 18, where the calculated neutron leakage current from the bare BeRP ball is shown. The Alpha79 library appears to overestimate the thermal neutron flux, which would tend to cause the Feynman-Y to be overestimated as well.

Summary

The Alpha79i cross-section library tends to produce approximately the same result as the Kynea3 library, except the former appears to estimate a much higher leakage current at thermal energies. This observation indicates that the Alpha79i library predicts a higher thermal neutron flux than the Kynea3 library. If this difference between the two libraries can be resolved in a subsequent revision of the Alpha79 series, then the Alpha79 should be suitable as a baseline for subsequent optimization studies.

Finally, it has been confirmed that the empirical model for detector efficiency has an incorrect shape, both near the cadmium cutoff and over the intermediate energy range. Those artifices were the cause for the overestimation of the Feynman-Y observed in previous tests.

Recommendations

University of Florida (UF) should seek to resolve the difference in the thermal flux estimated by the Alpha79i library relative to the Kynea3 library. Sandia may be able to assist UF by conducting laboratory measurements of moderated californium-252 using a detector sensitive to thermal neutrons.

Sandia should revise its procedure to unfold the empirical detector efficiency model to accurately reproduce the shape of the detection efficiency versus energy. In the meantime, Sandia should continue to use a detection efficiency calculated by MCNP. Sandia should revise its model of the NPOD multiplicity counter to include the effect of neutron reflection by the floor.

Tables and Figures

Table 1: Neutron multiplicity calculation metrics

Case	Reflector Thickness (mm)	k-effective			Multiplication			Count Rate (cps)			Feynman-Y Asmptote		
		Benchmark	Kynea3	Alpha79h	Benchmark	Kynea3	Alpha79h	Measured	Kynea3	Alpha79h	Measured	Kynea3	Alpha79h
berp0	0	0.781	0.753	0.753	4.6	4.1	4.0	8299	7909	7890	0.33	0.29	0.29
berp1	12.7	0.823	0.814	0.816	5.7	5.4	5.4	11133	11130	11250	0.55	0.54	0.55
berp2	25.4	0.864	0.863	0.867	7.4	7.3	7.5	14439	14760	15210	0.91	0.95	1.01
berp3	38.1	0.898	0.899	0.903	9.8	9.9	10.4	17488	17680	18520	1.42	1.50	1.65
berp4	76.2	0.935	0.936	0.939	15.5	15.6	16.4	14687	14200	14910	1.74	1.86	2.06
berp5	152.4	N/A	0.940	0.943	N/A	16.7	17.5	3646	2996	3109	0.47	0.44	0.48

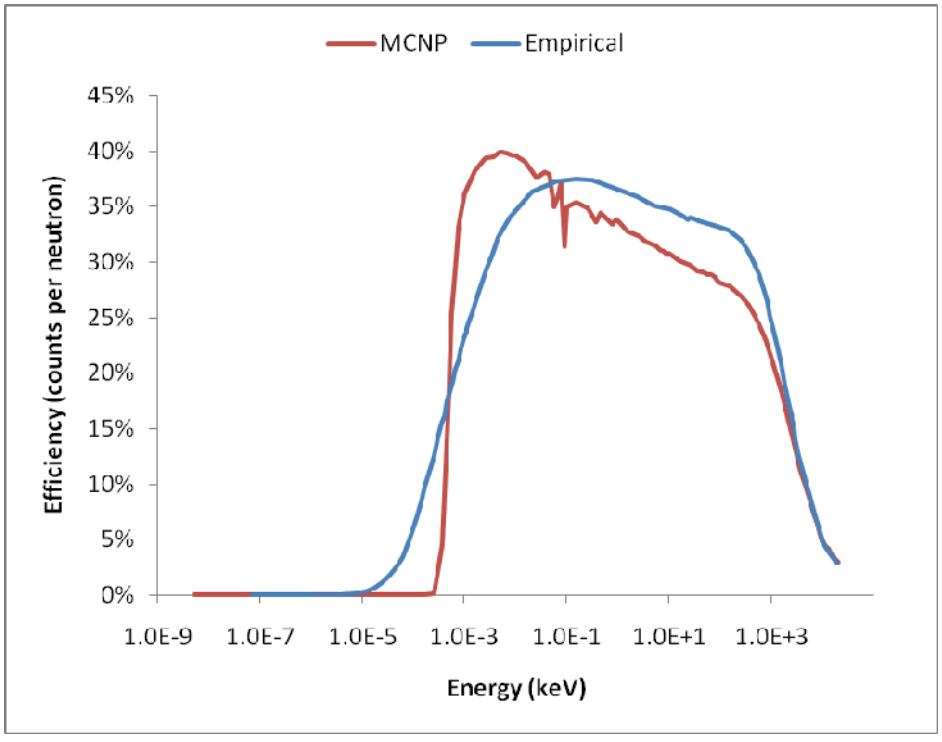

Figure 3: MCNP and empirical models of neutron detection efficiency

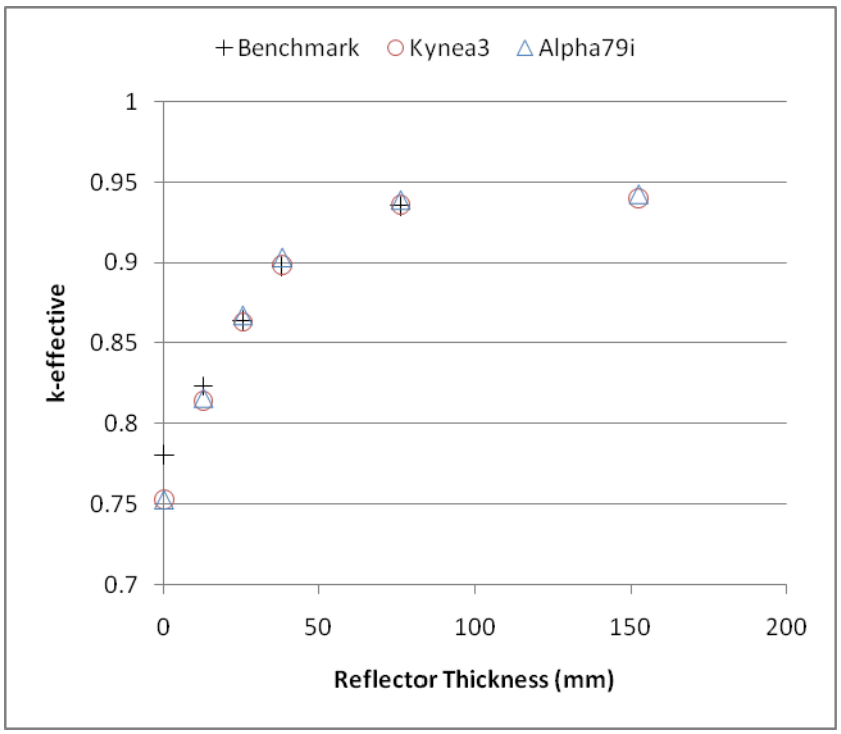

Figure 4: k-effective vs. polyethylene reflector thickness

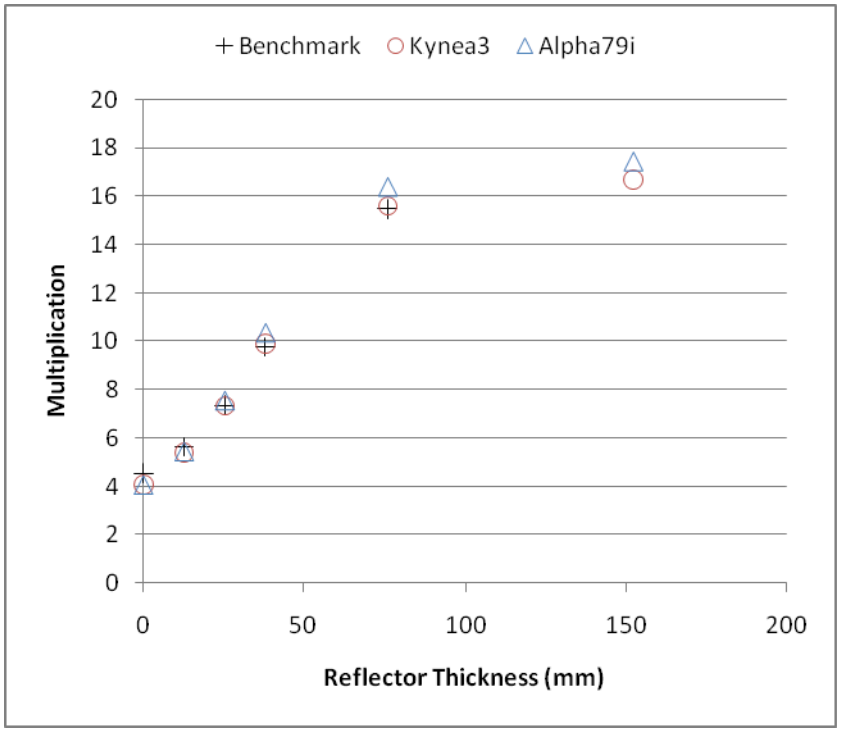

Figure 5: Multiplication vs. polyethylene reflector thickness

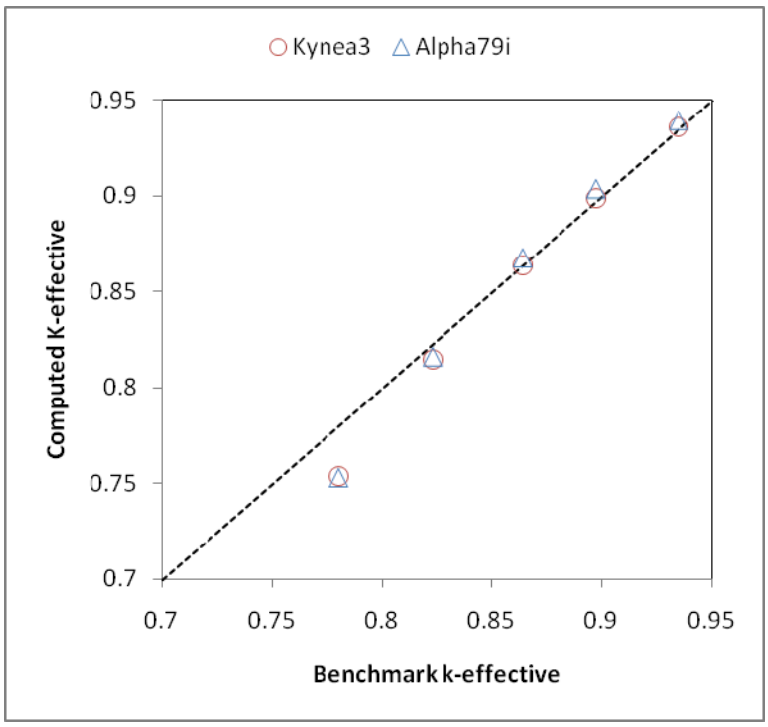

Figure 6: k-effective calculated by PARTISN vs. k-effective reported in Valentine's benchmark (Valentine 2008)

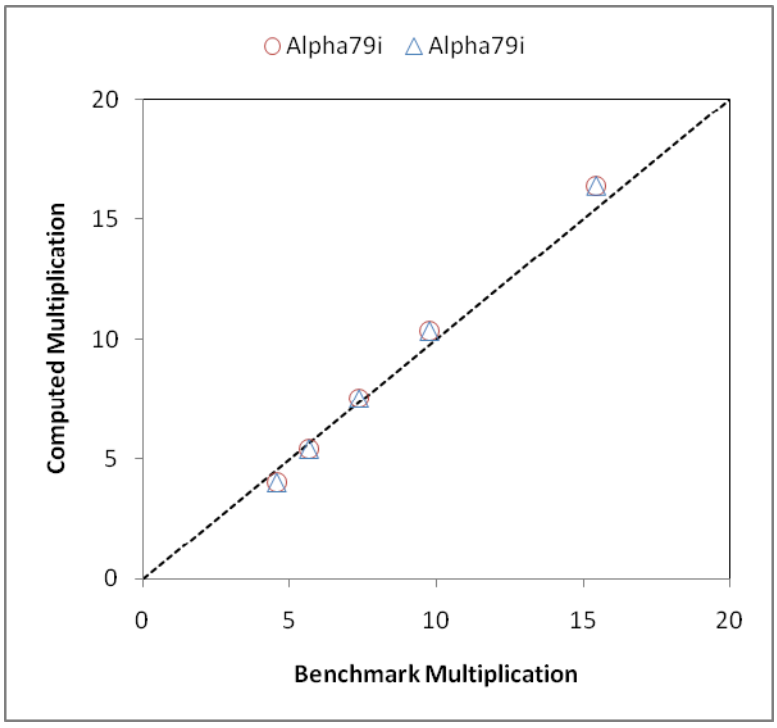

Figure 7: Multiplication computed by PARTISN vs. multiplication reported in Valentine's benchmark (Valentine 2008)

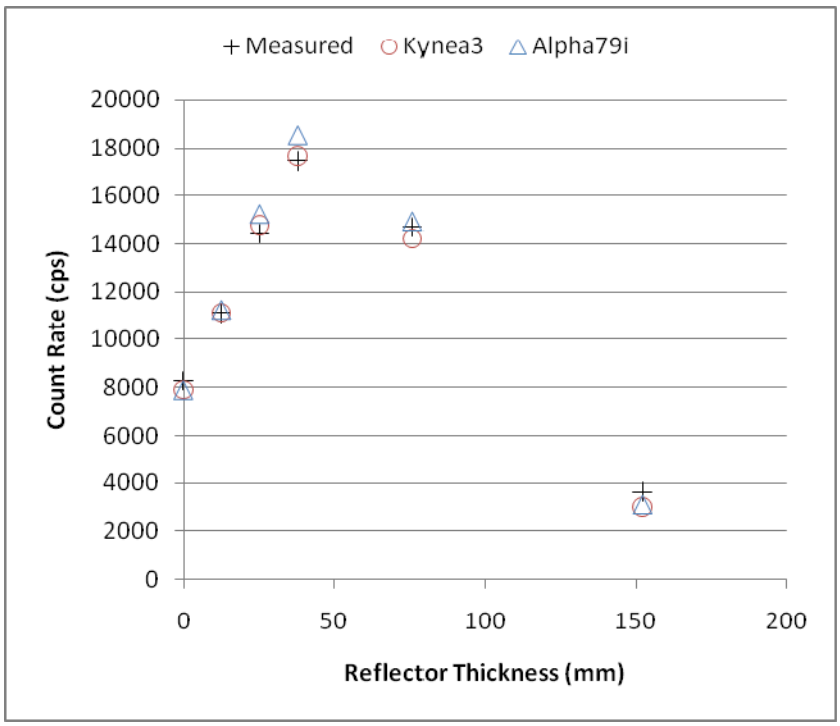

Figure 8: Count rate vs. polyethylene reflector thickness

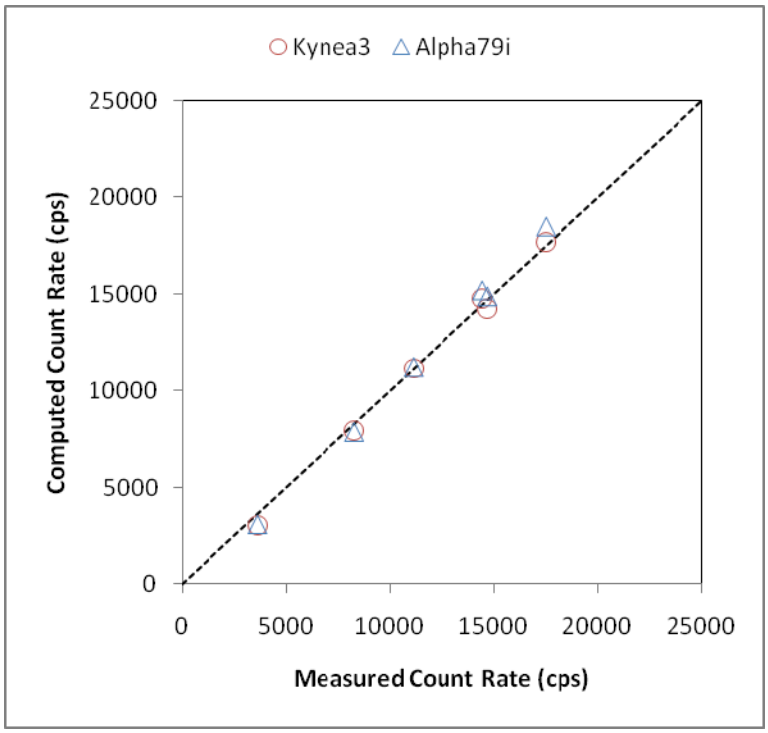

Figure 9: Computed count rate vs. measured count rate

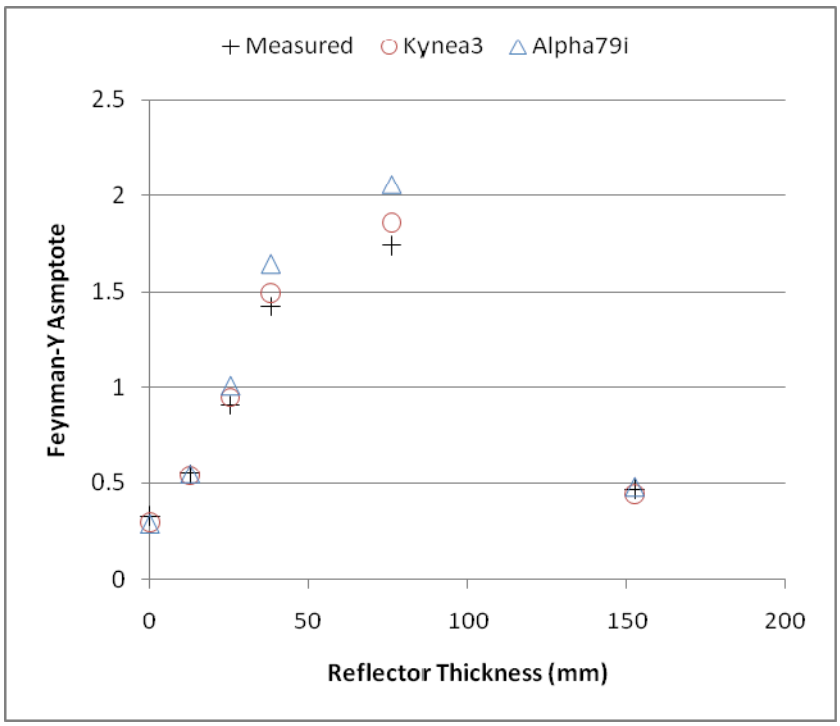

Figure 10: Feynman-Y asymptote vs. polyethylene reflector thickness

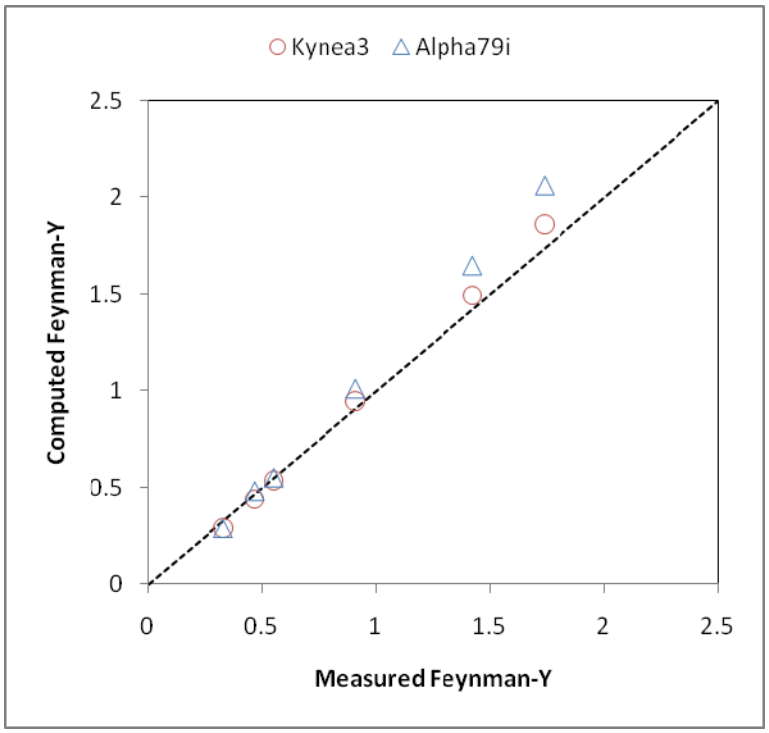

Figure 11: Computed Feynman-Y asymptote vs. measured Feynman-Y asymptote

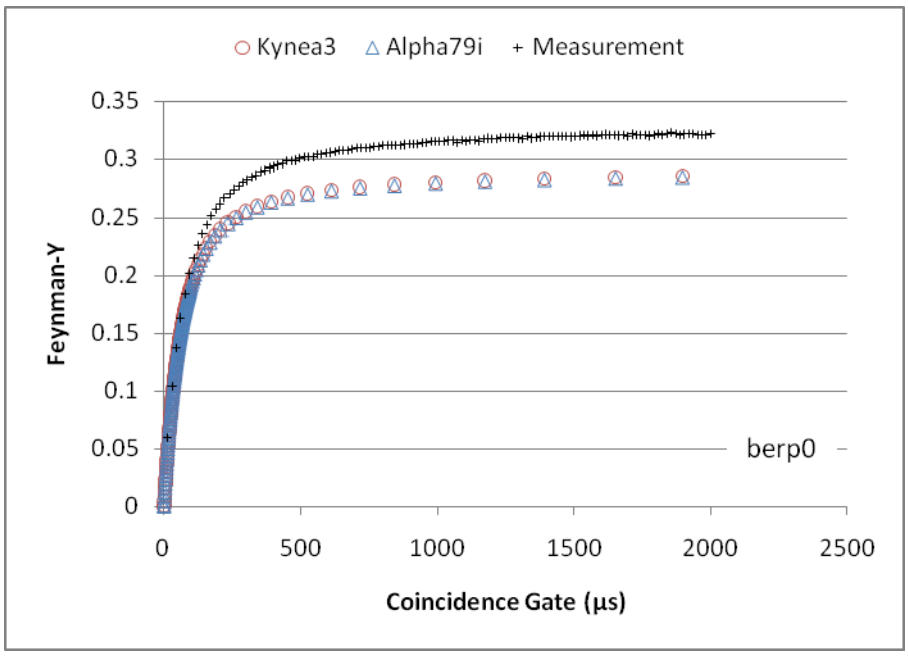

Figure 12: Calculated and measured Feynman-Y for the bare BeRP ball

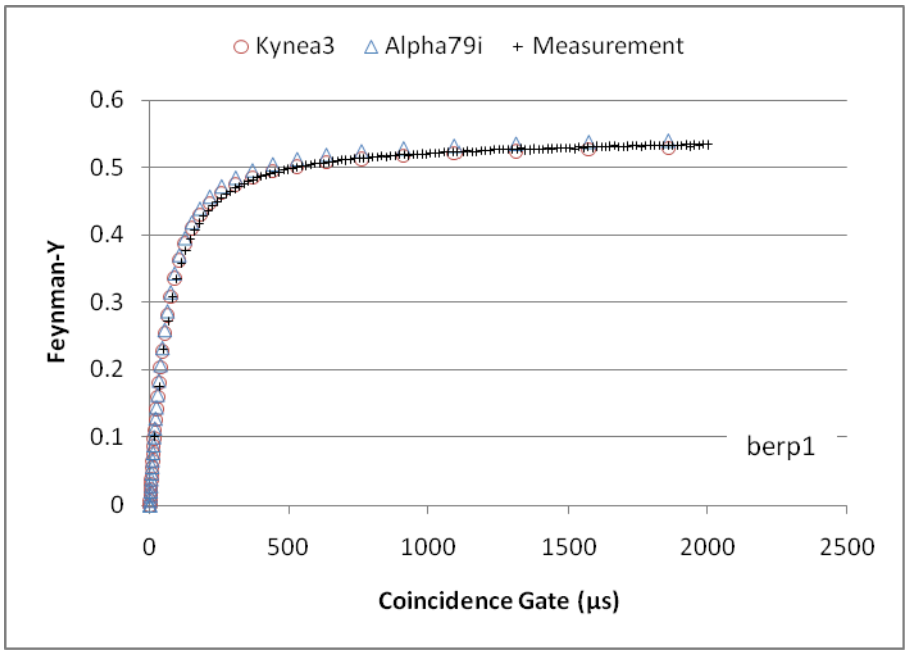

Figure 13: Calculated and measured Feynman-Y for the BeRP ball reflected by 12.7 mm of polyethylene

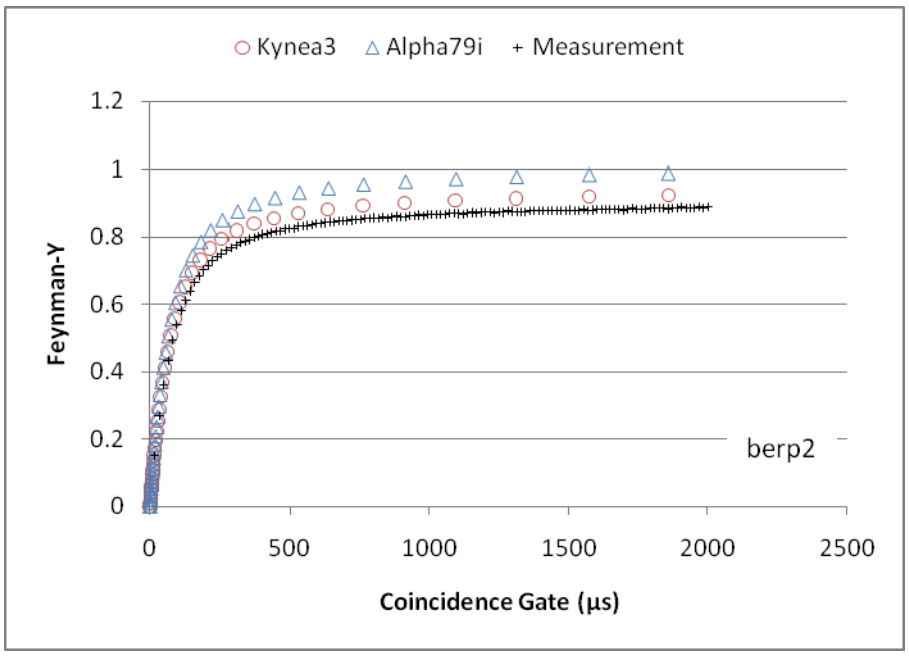

Figure 14: Calculated and measured Feynman-Y for the BeRP ball reflected by 25.4 mm of polyethylene

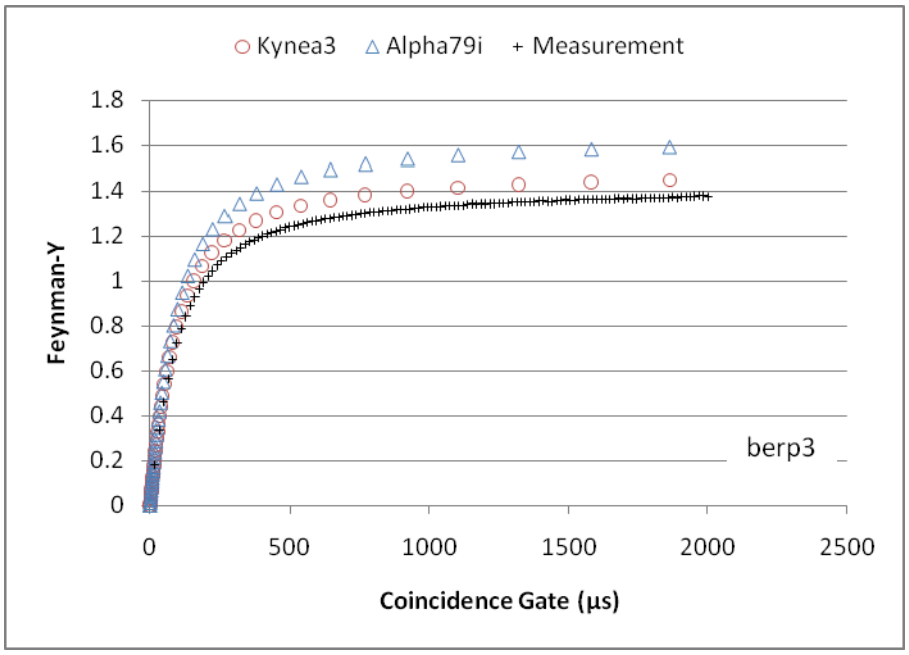

Figure 15: Calculated and measured Feynman-Y for the BeRP ball reflected by 38.1 mm of polyethylene

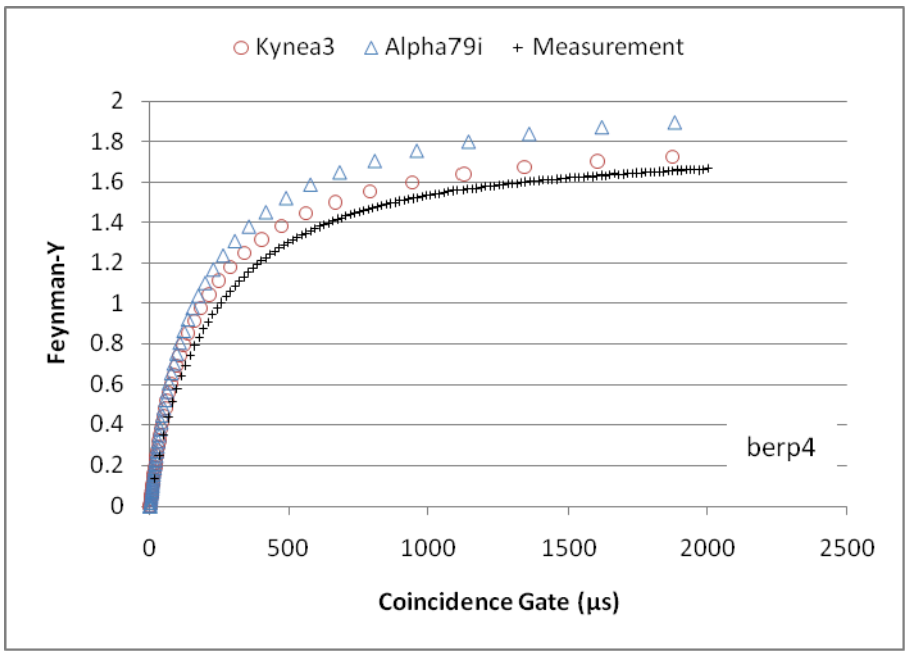

Figure 16: Calculated and measured Feynman-Y for the BeRP ball reflected by 76.2 mm of polyethylene

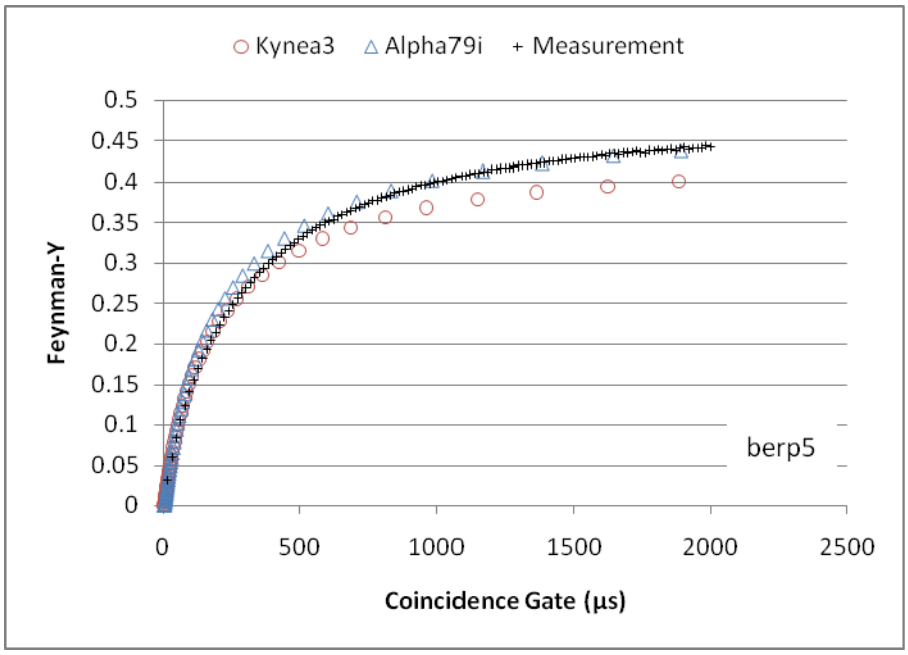

Figure 17: Calculated and measured Feynman-Y for the BeRP ball reflected by 152.4 mm of polyethylene

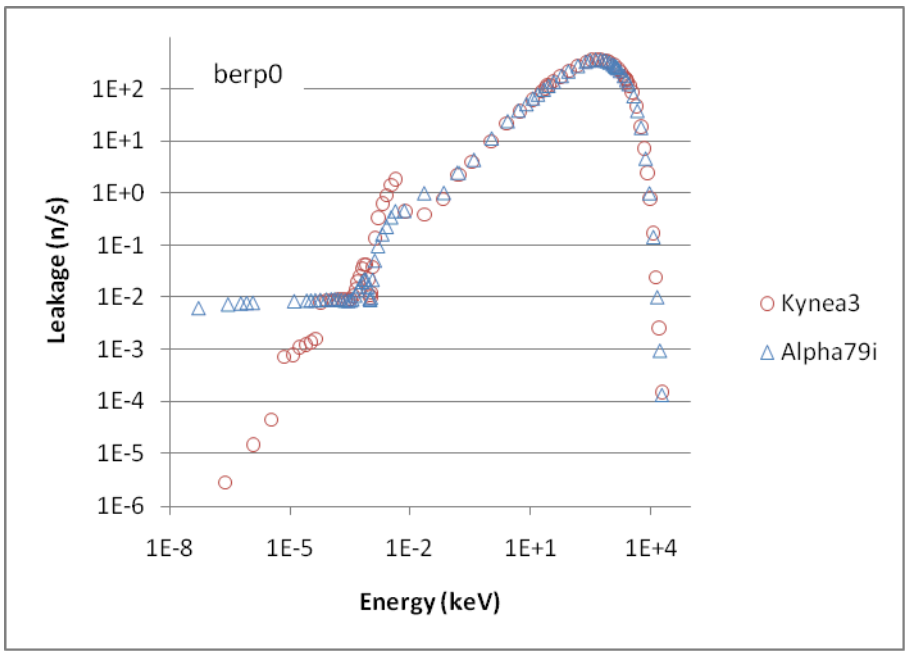

Figure 18: Calculated leakage spectra for the bare BeRP ball

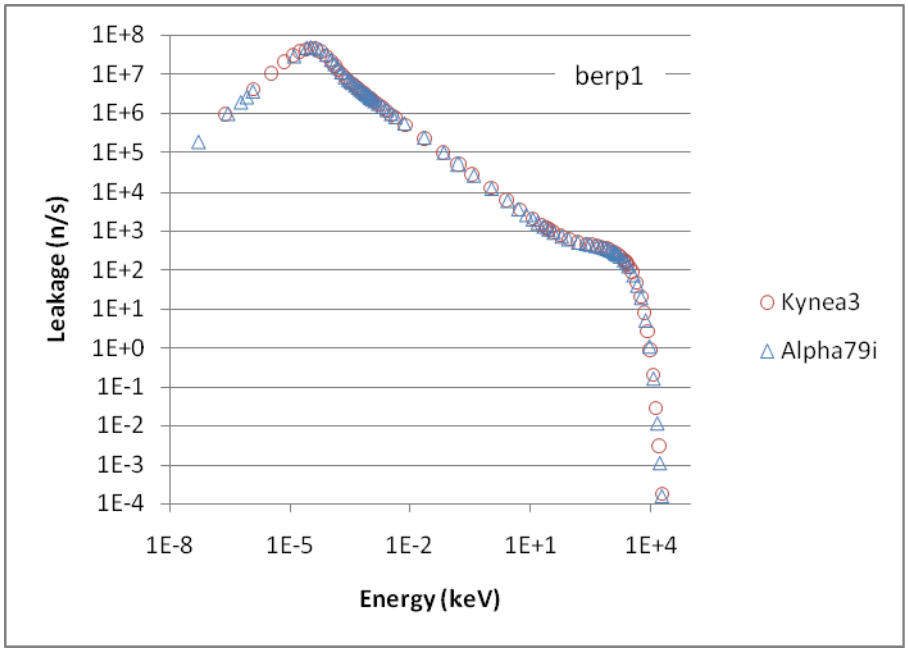

Figure 19: Calculated leakage spectra for the BeRP ball reflected by 12.7 mm of polyethylene

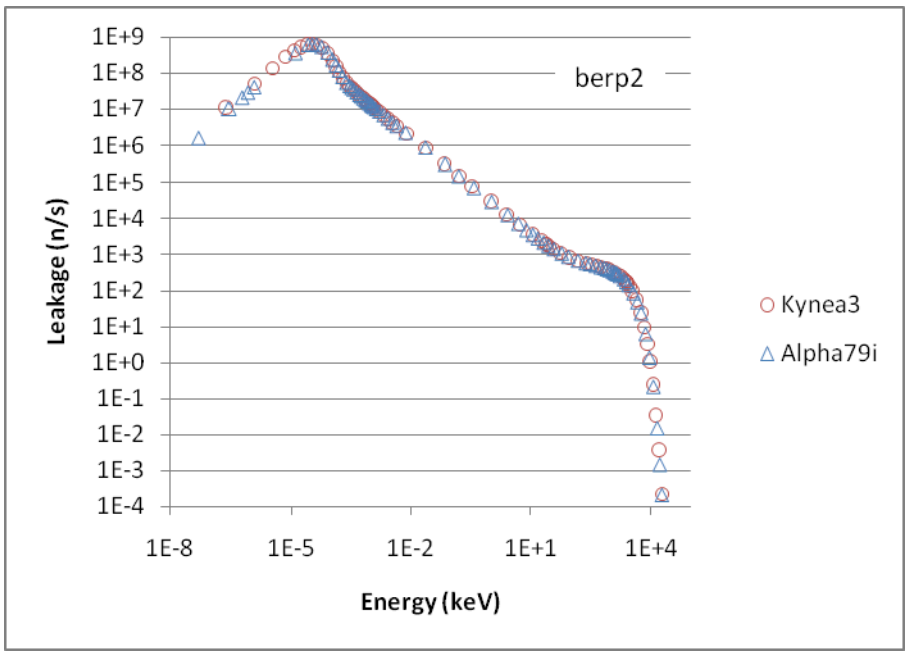

Figure 20: Calculated leakage spectra for the BeRP ball reflected by 25.4 mm of polyethylene

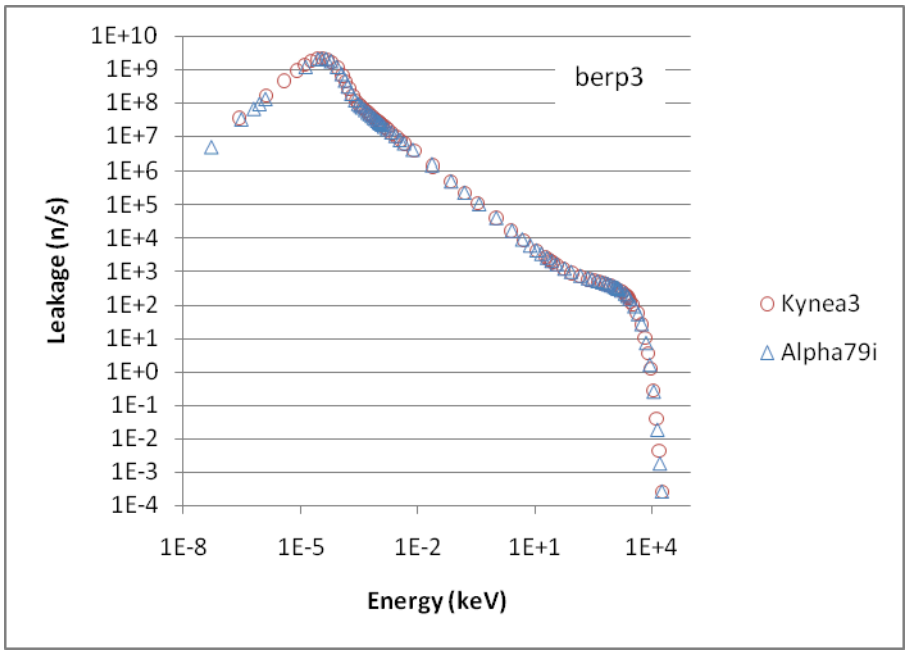

Figure 21: Calculated leakage spectra for the BeRP ball reflected by 38.1 mm of polyethylene

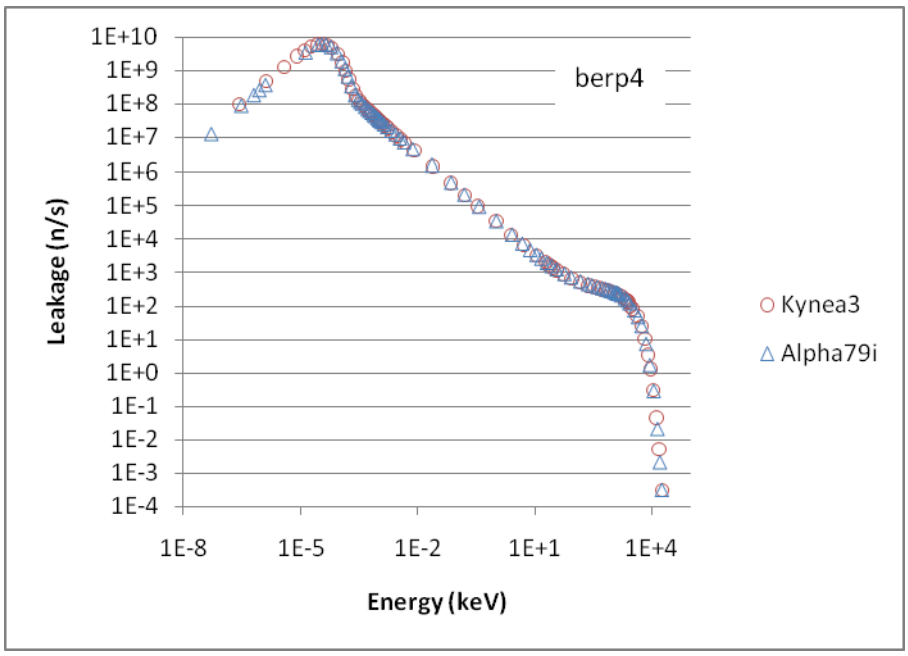

Figure 22: Calculated leakage spectra for the BeRP ball reflected by 76.2 mm of polyethylene

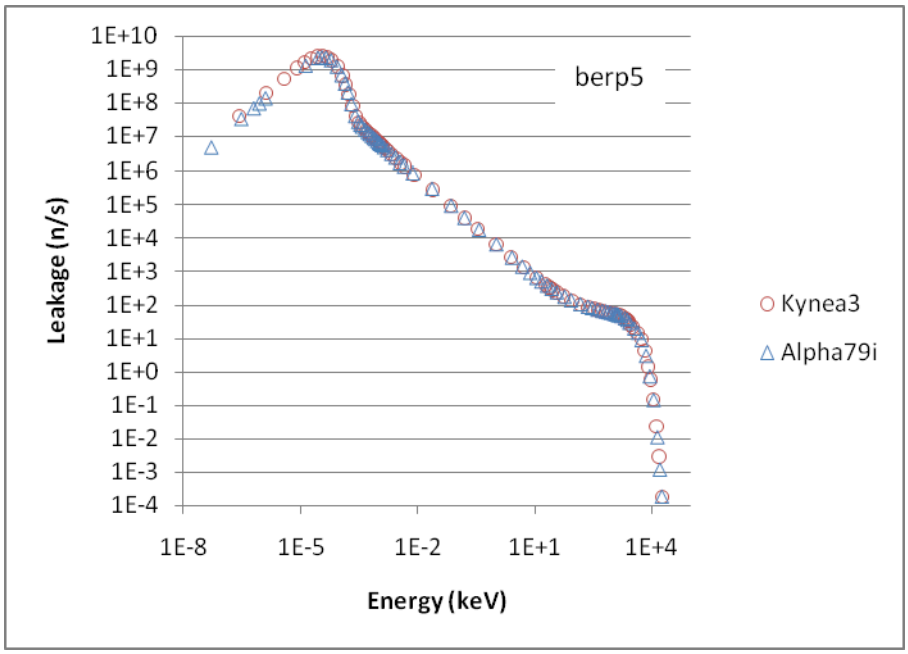

Figure 23: Calculated leakage spectra for the BeRP ball reflected by 152.4 mm of polyethylene

References

Bowman, S. M., M. E. Dunn, D. F. Hollenbach, and W. C. Jordan. *SCALE Cross-Section Libraries, ORNL/TM-2005/39 Version 5.1, Vol III, Section M4.* Oak Ridge National Laboratory, 2006.

Harding, Lee T., John Mattingly, and Dean J. Mitchell. *Modernized Neutron Efficiency Calculations for GADRAS, SAND2008-6073.* Sandia National Laboratories, 2008.

Mattingly, John. *BeRP Ball Reflected by Polyethylene: January 2009 Benchmarks, 2009-1832P.* Presentation, Sandia National Laboratories, 2009.

Mattingly, John. *MCNP Model of the Los Alamos Neutron Pod, 2009-2910P.* Presentation, Sandia National Laboratories, 2009.

Mattingly, John, and Eric S. Varley. "Synthesis of the Feynman-Y Neutron Multiplicity Metric using Deterministic Transport." *American Nuclear Society Transactions.* 2008. 572 - 574.

Valentine, Timothy E. "Polyethylene-Reflected Plutonium Metal Sphere Subcritical Noise Measurements, SUB-PU-MET-MIXED-001." In *International Handbook of Evaluated Criticality Safety Benchmark Experiments, NEA/NSC/DOC(95)03/I-IX*. Organization for Economic Co-operation and Development - Nuclear Energy Agency (OECD-NEA), 2008.

Varley, Eric S., and John Mattingly. "Rapid Feynman-Y Synthesis: Kynea3 Cross-Section Library Development." *American Nuclear Society Transactions.* 2008. 572 - 574.

White, J. E., R. Q. Wright, D. T. Ingersoll, R. W. Roussin, N. M. Greene, and R. E. MacFarlane. "VITAMIN-B6: A Fine-Group Cross-Section Library Based on ENDF/B-VI for Radiation Transport Applications." *International Conference on Nuclear Data for Science.* Organization for Economic Cooperation and Development - Nuclear Energy Agency (OECD-NEA), 1994. 733 - 736.